FYSC23

Powder X-ray Diffraction Lab

Authors
Fredrik Bergelv
Max Eriksson
`fredrik.bergelv@live.se`
`maxerikss@gmail.com`

LUND UNIVERSITY

March 3, 2025

Contents

1   Introduction

2   Theory

2.1   Crystal Lattice Structure

Crystal lattice structures are described by a Bravais lattice [1] which is an infinite array of points described by translational operations

$$\mathbf{R} = n_1 \mathbf{a}_1 + n_2 \mathbf{a}_2 + n_3 \mathbf{a}_3, \tag{1}$$

where $\mathbf{a}_i$ are the lattice vectors. Performing a Fourier transform of the real space lattice gives the reciprocal lattice in k-space, also a Bravais lattice, which is described by the reciprocal lattice vectors $\mathbf{b}_j$ defined by $\mathbf{a}_i \cdot \mathbf{b_j} = 2\pi \delta_{ij}$ [1]. The reciprocal lattice is useful when performing diffraction experiments since the diffraction pattern is in k-space.

To calculate the distance between planes the formula

$$\frac{1}{d^2} = \frac{h^2}{a^2} + \frac{k^2}{b^2} + \frac{l^2}{c^2} \tag{2}$$

is used. If we use this formula for a simple cubic with $a = b = c = 4.32 \times 10^{-1}$ nm for the plane(111) we get the separation to $d = 2.49 \times 10^{-1}$ nm. If we do the same for the plane (211) we obtain a separation of $d = 1.76 \times 10^{-1}$ nm and for the plane (100) we get $d = 4.32 \times 10^{-1}$ nm.

2.2   Diffraction

Diffraction is when light passes an obstacle, like an aperture, and the light deviates and spreads out [1]. In scattering experiments constructive and destructive interference can be observed which forms diffraction patterns that is analysed. Depending on the size of the obstacle, the wavelength of the light need to be chosen accordingly. For example, to resolve atomic structure the wavelength need to be on the same order as the lattice spacing, which is X-rays [1].

To evaluate diffraction patterns Bragg's law is mainly used, with is defined as

$$n\lambda = 2d \sin\theta, \tag{3}$$

where n is an integer, λ is the wavelength of the incoming photon, d is the spacing between the planes and θ is the scattering angle. Using this we see that if the incoming x-ray has a wavelength of 7×10^{-2} nm we can at minimum spacing which can be observed is 3.5×10^{-1} Å. In order to observe smaller spacings, a higher photon energy would have to be used.

For example if we have a (111) plane with an incident angle $\theta = 11.2°$ when X-rays of wavelength of 0.154 nm then the side of the side of each unit cell can be calculated as follows: From Equation 3 we obtain a the distance planer separation to $d = 3.97 \times 10^{-1}$ nm, from Equation 2 we obtain that a separation of $d = 3.97 \times 10^{-1}$ nm leads to a lattice constant of $a = 6.36$ Å for a simple cubic.

Another example for a orthorhombic unit cell with dimensions $a = 5.74$ Å, $b = 7.96$ Å and $c = 4.95$ Å one can calculate the incident angles for the (100), (010), and (111) planes if the wavelength is 8.3×10^{-2} nm. For the (100) plane Equation 2 gives a planar separation of $d_{(100)} = 5.74 \times 10^{-1}$ nm, (010) gives $d_{(010)} =$

7.96×10^{-1} nm and (111) gives $d_{(111)} = 3.39 \times 10^{-1}$ nm. Using Equation 3 the following angles are found: $\theta_{(100)} = 4.15°$, $\theta_{(010)} = 2.99°$ and $\theta_{(111)} = 7.03°$.

From Equation 3 we can derive the following:

$$\frac{d}{d\lambda}(n\lambda) = \frac{d}{d\lambda}(2d\sin\theta) \implies n = 2d\cos\theta\frac{d\theta}{d\lambda} = 2d\cos\theta\frac{\Delta\theta}{\Delta\lambda}, \tag{4}$$

using Bragg's law once again we obtain

$$\implies \frac{2d\sin\theta}{\lambda} = 2d\cos\theta\frac{\Delta\theta}{\Delta\lambda} \implies \Delta\theta = \frac{\Delta\lambda}{\lambda}\tan\theta. \tag{5}$$

This relation shows that the spectral contribution to the peak width θ is related to the spectral bandwidth $\Delta\lambda/\lambda$. However one must note that the broadening is also affected by other factors.

2.3 Structure Factors

Due to the structure of different types of lattices, the diffraction pattern may change. This is due to structure function which are defined as

$$F(hkl) = \sum_m f_m \exp\left(2\pi i(u_m h + v_m k + w_m l)\right). \tag{6}$$

where f_m is the atomic form factor and (u_m, v_m, w_m) are the fractional coordinates of atoms in the unit cell. for a bcc we know that we have the fractional coordinates (0,0,0) for each corner and (1/2,1/2,1/2). and for an fcc we have the (0,0,0) for each corner, (0,1/2,1/2), (1/2,0,1/2) and (1/2,1/2,0). In the equation above h,k,l is the value of the miller index. Putting all of this together we know that we will obtain diffraction peaks only if $F(hkl) \neq 0$ [2].

From this we can evaluate which planes we will see from bcc and fcc. From Equation 6 we can see that the points located at (0,0,0) will always yield a non-zero result. However, if we start looking at the bcc crystal we can obtain the following:

$$F(hkl) = f_m \exp\left[2\pi i\left(0h + 0k + 0l\right)\right] + f_m \exp\left[2\pi i\left(\frac{h}{2} + \frac{k}{2} + \frac{l}{2}\right)\right] = f_m\left[1 + \exp\left(2\pi i\frac{h+k+l}{2}\right)\right] \tag{7}$$

$$\text{if } F(hkl) \neq 0 \implies -1 \neq \exp\left(2\pi i\frac{h+k+l}{2}\right) \implies \frac{h+k+l}{2} \neq n + \frac{1}{2}, \text{ where n=1,2,3...} \tag{8}$$

$$\implies h + k + l \neq 2n + 1. \tag{9}$$

Above we used Euler's identity which says $\exp(i\pi(n+1/2) + 1 = 0$. We have thus shown that for the bcc structure wont show any planes where $h + k + l$ are odd. For the fcc we get the following instead:

$$F(hkl) = f_m + f_m \exp\left[2\pi i\left(\frac{h}{2} + \frac{k}{2}\right)\right] + f_m \exp\left[2\pi i\left(\frac{h}{2} + \frac{l}{2}\right)\right] + f_m \exp\left[2\pi i\left(\frac{k}{2} + \frac{l}{2}\right)\right] \tag{10}$$

$$\text{if } F(hkl) \neq 0 \implies -1 \neq \exp\left[2\pi i\left(\frac{h}{2} + \frac{k}{2}\right)\right] + \exp\left[2\pi i\left(\frac{h}{2} + \frac{l}{2}\right)\right] + \exp\left[2\pi i\left(\frac{k}{2} + \frac{l}{2}\right)\right] \tag{11}$$

As shown before, we can see above if one of h, k, l is even and the other are odd (or vice versa) then we get $-1 \neq 1 - 1 - 1$ which is not allowed. However if all h, k, l are even or odd we obtain $-1 \neq 1 + 1 + 1$ which is true. Thus the (h,k,l) is always all odd or all even for the fcc.

The order of the peaks we will see will be ordered as

$$\sqrt{h^2 + k^2 + l^2}, \tag{12}$$

where h, k and l are the miller indices of that specific plane. Thus, for a bcc crystal the peaks will be in the order (110), (200), (211), (220) and so on. For the fcc the peaks will be (111), (200), (220), (311), (222) and so on.

2.4   Powder X-ray Diffraction

Powder X-ray diffraction (PXRD) is a method of diffraction to analyse crystal structure. In PXRD the sample is a fine powder of many small crystallites instead of a single large crystal [1]. This means that the crystal planes will be randomly oriented, and all possible orientations will be present. The diffraction pattern will look like a series of rings, instead of sharp points which arises from single crystal diffraction [1]. One of the advantages of powder diffraction is that it is quicker than other methods of analysing crystal structures.

Transmission, fluorescence,

Xray diffraction, oscillating E field. When X ray hit the electrons the electrons start o vibrate in that frequency - Constructive and destructive interference

Bragg's law: $n\lambda = PD = 2s = 2d\sin\theta$

Crystal lattice: fcc, bcc

In powder diffraction we have all possible orientation sof the crystallites and some will be oriented in the right way for diffraction. Give rise to powder diffraction rings.

Scherrer's formula (Plz explain question 7 here)

$$t = \frac{k\lambda}{\beta\cos\theta} \tag{13}$$

Structure factor: Se photos. For a simple cubic we see all peaks, for bcc and fcc we loose some peaks.

3   Method

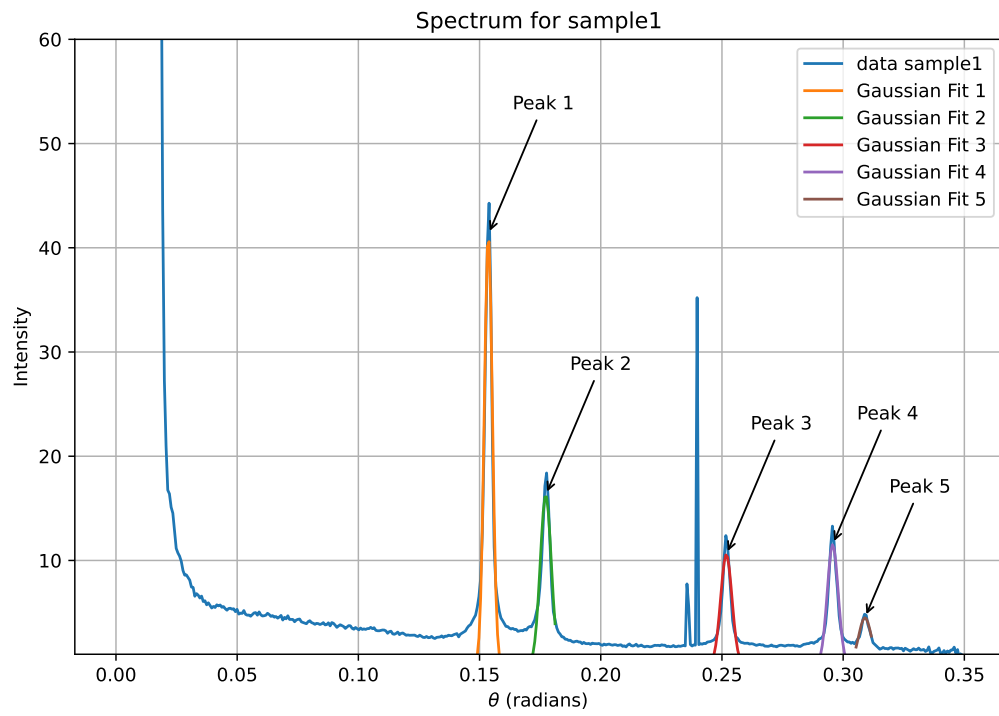The energy of the x-rays are 1.745×10^1 keV.

The detector uses six semiconductors.

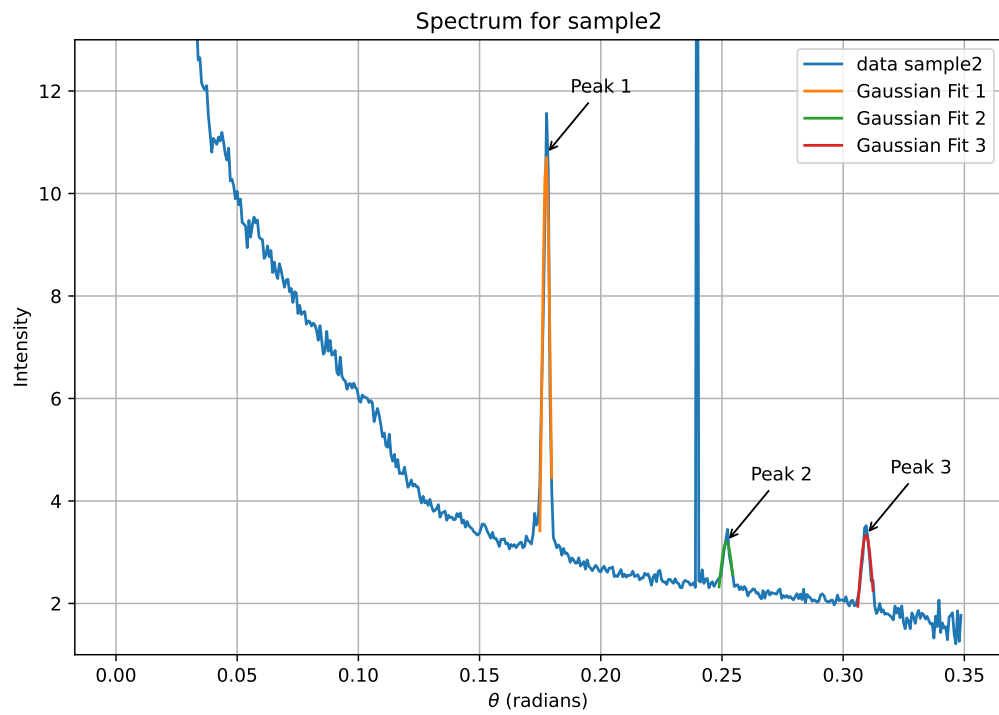Calibrations of hex.., this is good since we have a lot of diffraction rings.

1. Put in all the data 2. mask out dead spots 3. Tell where the rings are 4. The image is converted to an intensity plot (Note that the x-axis is in 2θ).

Hot pixel, high peak with no width. The pixel can be burnt out.

4 Result

(a) This is the first subfigure.

(b) This is the second subfigure.

Figure 1: This figure shows two subfigures with separate captions.

Table 1: Fitting results for Sample 1

Peak	Angle θ (radians)	Standard deviation σ (radians)	FWHM (radians)
Peak 1	$(1.5362 \pm 0.0010) \times 10^{-1}$	$(1.65 \pm 0.10) \times 10^{-3}$	$(3.88 \pm 0.23) \times 10^{-3}$
Peak 2	$(1.7731 \pm 0.0019) \times 10^{-1}$	$(2.27 \pm 0.20) \times 10^{-3}$	$(5.35 \pm 0.46) \times 10^{-3}$
Peak 3	$(2.5180 \pm 0.0018) \times 10^{-1}$	$(2.34 \pm 0.18) \times 10^{-3}$	$(5.50 \pm 0.43) \times 10^{-3}$
Peak 4	$(2.9569 \pm 0.0015) \times 10^{-1}$	$(2.25 \pm 0.15) \times 10^{-3}$	$(5.30 \pm 0.35) \times 10^{-3}$
Peak 5	$(3.0900 \pm 0.0015) \times 10^{-1}$	$(2.61 \pm 0.21) \times 10^{-3}$	$(6.16 \pm 0.49) \times 10^{-3}$

Table 2: Fitting results for Sample 2

Peak	Angle θ (radians)	Standard deviation σ (radians)	FWHM (radians)
Peak 1	$(1.7746 \pm 0.0012) \times 10^{-1}$	$(1.72 \pm 0.14) \times 10^{-3}$	$(4.04 \pm 0.34) \times 10^{-3}$
Peak 2	$(2.5186 \pm 0.0017) \times 10^{-1}$	$(3.80 \pm 0.39) \times 10^{-3}$	$(8.95 \pm 0.92) \times 10^{-3}$
Peak 3	$(3.0942 \pm 0.0014) \times 10^{-1}$	$(3.26 \pm 0.24) \times 10^{-3}$	$(7.68 \pm 0.56) \times 10^{-3}$

Using peak 1 from the first sample and $n = 1$, the plane (111) we obtain a spacing $a = (4.0213 \pm 0.0026)$ Å which coincides with the material Au using Equation 3 and Equation 2 with the given table [2]. The first peak coincides with the plane (111) as seen in Equation 12 and all indices are odd which is must be true since Au is a fcc. This verifies this result.

Using peak 2 from the second sample and $n = 1$, the plane (110) we obtain a spacing $a = (2.8484 \pm 0.0030)$ Å which coincides with the material Fe using Equation 3 and Equation 2 with the given table [2]. The second peak coincides with the plane (110) as seen in Equation 12, also the sum of the miller indices is even which must be tru for a bcc such as Fe, verifying this result.

Using Equation 13, we obtain the following particle sizes as shown in Table 3 and Table 4. The mean particle size for Sample 1 is (13.44 ± 0.04) nm, and for Sample 2, it is (11.2 ± 0.6) nm.

Table 3: Powder size t for Sample 1

Peak	Size (m)
Peak 1	$(1.74 \pm 0.10) \times 10^{-7}$
Peak 2	$(1.27 \pm 0.11) \times 10^{-7}$
Peak 3	$(1.25 \pm 0.10) \times 10^{-7}$
Peak 4	$(1.32 \pm 0.09) \times 10^{-7}$
Peak 5	$(1.14 \pm 0.09) \times 10^{-7}$

Table 4: Powder size t for Sample 2

Peak	Size (m)
Peak 1	$(1.68 \pm 0.14) \times 10^{-8}$
Peak 2	$(7.7 \pm 0.8) \times 10^{-9}$
Peak 3	$(9.1 \pm 0.7) \times 10^{-9}$

5   Discussion

In Figure 1, we can identify the peaks using the theory derived above. Since we know that Sample 1 was gold, which has an FCC structure, the first peak corresponds to the (111) plane, the second peak to the (200) plane, the third peak to the (220) plane, the fourth peak to the (331) plane, and the fifth peak to the (222) plane. For the second sample, we know that the material was iron with a BCC structure. This means that the first peak corresponds to the (110) plane, the second peak to the (200) plane, and the third peak to the (211) plane.

The mean size of the gold and Fe powders also seems plausible. It is interesting to note that the iron

powder was smaller than the gold powder. Both of these values, however, fall within a reasonable range for powder materials. There was also some variation in the powder size, which is expected since not all particles are exactly the same size.

In Equation 5, it was shown that the spectral contribution of the X-ray source to the peak width was related to the spectral bandwidth. However, other factors also contribute to instrumental broadening, such as the width of the X-ray beam, beam divergence, and the resolution of the detector. Additional broadening effects arise due to disorder of the second kind, where atomic fluctuations cause variations in the distances between neighboring atoms. This leads to peak broadening and a decrease in peak height [3]. This effect becomes more pronounced at increasing angles, meaning that it has a greater impact on higher-order peaks.

6   Conclusion

References

[1] Philip Hofmann. *Solid State Physics: An Introduction*. Wiley-VCH, 2nd edition, 2015.

[2] Auden Ti and Hajar Jalili. *FYSC23: Powder X-ray Diffraction Laboratory Manual*. Lund, 2025. Lab instructors: Auden Ti (`auden.ti_yun@sljus.lu.se`) and Hajar Jalili (`hajar.jalili@sljus.lu.se`).

[3] A. Guinier. *X-Ray Diffraction*. WH Freeman, San Francisco and London, 1963.